



UNIVERSITY OF LEEDS

This is a repository copy of *Metabolism of polysaccharides in dynamic middle lamellae during cotton fibre development*.

White Rose Research Online URL for this paper:
<http://eprints.whiterose.ac.uk/142664/>

Version: Accepted Version

Article:

Guo, X, Runavot, J-L, Bourot, S et al. (8 more authors) (2019) Metabolism of polysaccharides in dynamic middle lamellae during cotton fibre development. *Planta*, 249 (5). pp. 1565-1581. ISSN 0032-0935

<https://doi.org/10.1007/s00425-019-03107-4>

© 2019, Springer-Verlag GmbH Germany, part of Springer Nature. This is a post-peer-review, pre-copyedit version of an article published in *Planta*. The final authenticated version is available online at: <https://doi.org/10.1007/s00425-019-03107-4>. Uploaded in accordance with the publisher's self-archiving policy.

Reuse

Items deposited in White Rose Research Online are protected by copyright, with all rights reserved unless indicated otherwise. They may be downloaded and/or printed for private study, or other acts as permitted by national copyright laws. The publisher or other rights holders may allow further reproduction and re-use of the full text version. This is indicated by the licence information on the White Rose Research Online record for the item.

Takedown

If you consider content in White Rose Research Online to be in breach of UK law, please notify us by emailing eprints@whiterose.ac.uk including the URL of the record and the reason for the withdrawal request.



eprints@whiterose.ac.uk
<https://eprints.whiterose.ac.uk/>

Metabolism of polysaccharides in dynamic middle lamellae during cotton fibre development

Xiaoyuan Guo¹, Jean-Luc Runavot², Stéphane Bourot², Frank Meulewaeter², Mercedes Hernandez-Gomez⁴, Claire Holland¹, Jesper Harholt¹, William G.T. Willats³, Jozef Mravec¹, Paul Knox⁴ and Peter Ulvskov¹

1: Copenhagen University, Department of Plant and Environmental Sciences, Frederiksberg, Denmark

2: Bayer CropScience NV - Innovation Center, Technologiepark 38, 9052 Gent, Belgium.

3: School of Agriculture, Food and Rural Development, Newcastle University, Newcastle upon Tyne, NE1 7RU, UK.

4: Centre for Plant Sciences, Faculty of Biological Sciences, University of Leeds, Leeds LS2 9JT, UK.

Main conclusion: Evidence is presented that cotton fibre adhesion and middle lamella formation are preceded by cutin dilution and accompanied by rhamnogalacturonan-I metabolism.

Abstract

Cotton fibres are single cell structures that early in development adhere to one another via the cotton fibre middle lamella (CFML) to form a tissue-like structure. The CFML is disassembled around the time of initial secondary wall deposition, leading to fibre detachment. Observations of CFML in the light microscope have suggested that the development of the middle lamella is accompanied by substantial cell wall metabolism but it has remained an open question as to which processes mediate adherence and which lead to detachment. The mechanism of adherence and detachment were investigated here using glyco-microarrays probed with monoclonal antibodies, transcript profiling, and observations of fibre auto-digestion. The results suggest that adherence is brought about by cutin dilution, while the presence of relevant enzyme activities and the dynamics of rhamnogalacturonan-I side-chain accumulation and disappearance suggest that both attachment and detachment are accompanied by rhamnogalacturonan-I metabolism.

Keywords: Arabinofuranosidase, Cuticle, Post genital fusion, Rhamnogalacturonan-I, Xyloglucan

Abbreviations: CDTA 1,2-cyclohexanediamine-tetraacetic acid

CFML Cotton fibre middle lamella

CoMPP Comprehensive Microarray Polymer Profiling

DPA Days post anthesis

Funding: This work was supported by Villum Foundation project PLANET (grant no. 00009283) and the European Union Seventh Framework Programme under the WallTraC project (grant agreement No. 263916). This paper reflects the authors' views only. The European Community is not liable for any use that may be made of the information contained herein. The funders had no role in study design, data collection and analysis, decision to publish, or preparation of the manuscript.

Introduction

Plant cells expand with constant primary wall thickness, if carbon is not limited, and is accompanied by the deposition of new wall material (McCann and Roberts 1994).

Cessation of expansion and wall maturation may be accompanied by the deposition of a secondary wall on the inside of the primary wall, leading to an increase in wall thickness. It is now well established that primary and secondary wall biosynthesis is catalysed by separate gene modules (Ruprecht et al. 2011) and the first insight into the underlying regulatory networks is emerging, see review by Li et al. (2016).

Cotton fibres are single cell seed trichomes and are an excellent model for the study of cell wall biosynthesis, including the transition from primary to secondary wall deposition (Zhong et al. 2001; Haigler et al. 2012). However, the fibres are very specialised cells and cannot be regarded a general model for the study secondary wall deposition (MacMillan et al. 2017). Moreover there are unique cell attachment and cell detachment processes during fibre development.

Four developmental stages are recognized: initiation, elongation, thickening, and maturation (Kim and Triplett 2001). Each cotton fibre is a single and phenomenally elongated cell that originates from the epidermal layer of the ovule. These single fibre cells, developing near synchronously, elongate and eventually produce a thick cell wall consisting of more than 94% cellulose (Yang et al. 2008). Even though the fibres are made up largely of cellulose, other less abundant polysaccharides are important in ways that may be specific to cotton fibre cells. For example, developing cotton fibres transiently synthesise callose at the onset of secondary wall deposition (Maltby et al. 1979) and Hernandez-Gomez et al (2015a) found xylan and cellulose transcript abundance to be tightly correlated during fiber development.

The elongating trichomes initially adhere in a tissue-like fashion mediated by a structure called the cotton fibre middle lamella (CFML; Singh et 2009). The biological significance of the CFML is not well understood. This trichome surface layer does not originate from the cell plate, as the name “middle lamella” would imply (Jarvis et al. 2003), but instead is the result of post-differentiation fusion. Cell fusion is not common in plants but has long been recognised to play a role in, for example, gynoecium formation (Verbeke 1992) and post-genital fusion of other floral organs (Zhong and Preston 2015). This process generally comprises dissolution of the cutin layer, exchange of as yet unidentified signaling molecules, de-differentiation of epidermal cells, and occasionally the formation of new plasmodesmata (van der Shoot et al. 1995). De-differentiation is obviously not at play in post-genital fusion of cotton fibres and no plasmodesmata were observed by transmission electron micrographs presented by Singh et al. (2009). These authors noted the absence of a cutin layer as the main commonality between fibre fusion and the mechanisms of other post-genital fusion processes.

Middle lamella dissolution and fibre detachment coincide with the onset of secondary wall deposition. Middle lamella dissolution would be expected to be accompanied by expression of polysaccharide degrading enzymes while the preceding phase of cell elongation would be expected to be accompanied by the broader class of wall-remodeling enzymes and non-catalytic proteins, like expansins. Experimental data has been presented to support this expectation: Literature on cotton fibres has repeatedly reported gene upregulation and peak activities of cell wall remodelling enzymes during fibre elongation (Shimizu et al. 1997; Orford and Timmis 1998; Michailidis et al. 2009), and xyloglucan endotransglycosylase activity has been observed to be particularly high during the elongation phase and decline during the transition phase (Shao et al., 2011).

A detailed immunohistochemical investigation of CFML by Hernandez-Gomez et al. (2017) revealed the occurrence of bulges in the CFML that appeared as pairwise spots in one cultivar (FM966) but were present in all of four varieties investigated. It is not altogether clear whether these bulges represent points of adherence involved in post-genital fusion, or whether they alternatively mark the onset of CFML dissolution eventually leading to detachment. What was observed by Hernandez-Gomez et al. (2017) was that xyloglucan accumulated and the arabinan epitope LM13 disappeared

from the paired cell wall bulges, coinciding with the transitional phase preceding secondary cell wall deposition and fibre detachment. Cell wall polymer dynamics is affected by both the rate of deposition and the rate of degradation. The biosynthesis of cellulose and the main hemicellulosic polysaccharides in cotton fibre, mannan and xylan, has been investigated by Hernandez-Gomez et al. (2015a) while biosynthesis of cutin, xyloglucan and pectic polysaccharides of relevance to the CFML are the topics of the present report.

Materials and methods

Plant material

Five cotton cultivars from four different *Gossypium* species were analysed in this study, *G. hirsutum* (cv FM966), *G. barbadense* (cv China10 and cv PimaS7), *G. arboreum* (cv 30834 and cv JFW15) (Bayer CropScience). Cotton plants were grown under constant conditions at 28°C / 26°C (16h / 8h) day / night temperature cycle in phytotron greenhouse. Cotton flowers were tagged on the day of anthesis which enabled the cotton bolls to be harvested at the definite timepoints, days post anthesis (DPA). Collected cotton bolls were frozen in liquid nitrogen after harvest and stored at -20°C. For the Comprehensive Microarray Polymer Profiling (CoMPP) experiment determining relative cell wall compositions, fibres detached from the cotton bolls from at least three different plants were pooled together and boiled in 70% (v/v) ethanol for 30 min. After air-dry fibres were homogenised using nitrogen-cooled crushers (SPEX Sample Prep Freezer/mill 6870). For the RNA sequencing (RNA-seq) analysis, fibres were detached from five bolls from different plants on dry ice for each cotton line. The cotton bolls used for transcriptomic analysis were stored at -80°C until extraction.

Comprehensive Microarray Polymer Profiling (CoMPP)

CoMPP analysis was carried out as previously described (Moller et al. 2007). Two diploids, cv30834 and cvJFW15, and two tetraploids, cvPimasS7 and cvFM966 were selected for this analysis. For each three weighing replicates 10 mg of grounded fine cotton fibre powder was extracted in two 300 µl solvents sequentially, 50 mM 1,2-cyclohexanediamine-tetraacetic acid (CDTA) and 4M NaOH with 1% (v/v) NaBH₄ for pectic polysaccharides epitope extraction and hemicellulose and more tightly bonded polymers, respectively. After 2 h extraction with shaking and 3000 g centrifugation for 15 min, supernatants were printed in four printing replicates and four dilutions in ratio of 1:2, 1:6, 1:18 and 1:54 [v/v], giving a total of 48 spots representing each time point for each solvent on one array. Three independent prints and three independent probings of each print, giving total nine technical replicates, were applied in the data analysis. CoMPP results were presented by individual scaling in which maximum signal observed in each probe was assigned as 100 and the other signals scale to the highest value. Line chart was generated by plotting individual scaled CoMPP data and there is one 100 value in each probe chart. The CoMPP technique is a semi-quantitative method which only provides information of relative amount of solvent extractable epitopes.

Microscopy

Resin sections were used for immunofluorescence detection of cell wall epitopes. PBS with 5% (w/v) milk protein was added for 30 min at room temperature to prevent non-specific binding. Primary antibodies were used at a 1:5 dilution in 5% milk/PBS for 1.5 h. Anti-mouse or ant-rat IgG Alexa Fluor488 (Life Technologies) were used as secondary antibodies in a 1:100 dilution in 5% milk/PBS and samples were incubated for 1 h. Calcofluor White (Sigma–Aldrich) was used at 0.02 mg/ml in PBS for 5 min for

visualisation of cell walls. Anti-fade reagent Citifluor glycerol/PBS (Agar Scientific) was used to mount slides. Immunofluorescence imaging was performed using an Olympus BX61 microscope (<http://www.olympus-global.com/>) equipped with epifluorescence irradiation. Micrographs were obtained with a Hamamatsu ORCA285 camera (Hamamatsu, <http://www.hamamatsu.com>) and PerkinElmer Volocity software. All related and comparative micrographs were captured using equivalent settings, and relevant micrographs were processed in equivalent ways for the generation of datasets. In all cases the area shown in each micrograph is representative of the fibre tissue seen in at least 3 sections analysed from one plant. In the case the FM966 line the micrographs are representative of the analysis of more than 3 plants.

Transcriptomic analysis

Transcriptomic profiles were derived from the same dataset that formed the basis for the analysis of cellulose, mannan and xylan biosynthesis by Hernandez-Gomez et al. (2015a). Cotton species and cultivars were selected to cover variation in ploidy number and fibre properties. Annotation of transcripts in this dataset was carried out by mapping contigs to the *Gossypium raimondii* proteome. Levels of expressions were normalised to the total number of transcripts in the dataset for each variety. Transcript abundance of interest to the present study varied over ~2 orders of magnitude and were arbitrarily scaled so that the rarest transcript, the one mapping to the xyloglucan fucosyltransferase, is displayed on a y-axis of scale = 1, and more abundant transcripts on y-axes scaled relative to the fucosyltransferase.

Orthology was established on the basis of sequence similarities between the *G. raimondii* protein sequences and annotated proteins from mainly *Arabidopsis thaliana*, Table 2.

Polysaccharide hydrolase assays and autolysis

While CoMPP, microscopy and transcriptomics were carried out on the same sample set, the biochemical assays were devised in view of the transcriptomics and CoMPP analyses and were thus carried out later and also under different conditions. Plants were grown in glasshouses under ambient lighting and capsules were collected across the growing season. Synchrony with the transcriptomics studies was not attempted and time courses are not reported. Capsules were collected in the 15-26 DPA range and those with locular sap were selected for analysis. Reported measurements are means of triplicates.

Enzyme extraction

Locular sap was used directly. 700 mg of fibres were collected into 700 μ l 5 mM NaOAc pH= 5.5 with triple strength Complete (protease inhibitor cocktail, Sigma-Aldrich). Three 3 mm glass beads were added and the vial was treated for 30 sec, in the tissuelyser at 30 strokes per sec. The fibres are not homogenised by this treatment. Centrifugation for 10 min at 25000 g. The supernatant is referred to as the buffer extract. 25 ml of ice-cold H₂O was added, vortexed and centrifuged 10 min at 3000 g. This wash was discarded. 250 μ l buffer and 500 μ l 2 M LiCl was added to the fibres followed by 30 min of agitation on a rocking table at 4°C. The supernatant following 10 min centrifugation at 25000 g is referred to as the LiCl-extract.

p-nitrophenyl- α -arabinofuranoside was used as substrate at 4 mM in 5 mM NaOAc pH= 5.5 (the approximate pH of the locular sap). The reaction was terminated with an equal volume of 0.5 M Na₂CO₃ followed by absorbance measurement at 405 nm.

Substrates, potato RG-I prepared according to Byg et al. (2012), gum Arabic (Sigma) and larch arabinogalactan (Megazyme) were desalted on a NAP10 column. Desalted stock concentration 15 mg/ml. Arabinohexafuranose (Megazyme) was used directly. 25 μ l of water (background) or substrate stock containing 375 μ g polysaccharide was added to 100 μ l of desalted enzyme extract and incubated overnight (ON) and then analysed using the Megazyme enzyme coupled Ara+Gal assay kit following the supplier's instructions.

Autolysis

Freshly harvested fibres were washed in icecold water and incubated in NaOAc buffer on a rocking table at room temperature ON (autolysis). ~100 mg fibres/ml of buffer. The supernatant was hydrolysed (2M trifluoroacetic acid, 110 °C for 1 h) and analysed for monosaccharides according to Øbro et al. (2004).

Results

Transition to secondary wall deposition in cotton fibre

Cotton fibre development is biphasic: An elongation phase that precedes secondary cell wall deposition followed by secondary cell wall biosynthesis. Soluble callose may be used as a marker of the transition to secondary wall deposition (Maltby et al. 1979), whereas the callose fraction that requires NaOH for extraction is more uniformly present throughout development. Glyco-microarrays probed with monoclonal antibodies (CoMPP) are well suited to determine relative abundance and extractability. The polysaccharide fraction extracted with the calcium chelator CDTA is enriched in polymers that are not tightly bound, directly or indirectly to cellulose. Following CDTA extraction 4M NaOH is used to extract tightly bound polysaccharides. Sequentially extracted callose is shown in Fig. 1 corroborating that the abundance of less tightly bound callose peaks around the time of transition to secondary wall synthesis. Synchronisation across the four varieties was pronounced but not perfect.

Cellulose biosynthesis as a marker for secondary wall deposition

Due to the insolubility of cellulose in extraction solvents used in CoMPP, cellulose cannot be reliably analysed in this way. Carbohydrate binding module CBM3a has a high affinity for cellulose but also some low affinity recognition of xyloglucan, see Hernandez-Gomez et al. (2015b) for a discussion. Instead, cellulose biosynthetic genes may be used as markers for accumulation since cellulose is unlikely to be turned over. Korrigan (KOR), a membrane-bound β -glucanase, is involved in cellulose biosynthesis (Nicol et al. 1998; Mølhøj et al. 2001) presumably as a proofreading enzyme in microfibril assembly. KOR expression levels (Fig. 2) indicate a progression of cellulose biosynthesis as observed in earlier studies (Tuttle et al. 2015; MacMillan et al. 2017). The synchrony across cotton lines is not perfect. Previous investigations of this data set found transcript accumulation of cellulase synthase genes to rise most rapidly in JFW15 (Hernandez-Gomez et al. 2015a) and this is corroborated by the KOR expression profiles.

Cutin biosynthesis

Fig. 2 additionally displays expression profiles of cutin synthase and a number of transcription factors known to be inducers of cutin biosynthesis (Fich et al. 2016). Transcripts corresponding to shine1, 2 and 3 transcription factors, which are also implicated in cutin biosynthesis, were detected (data not shown) but at much lower levels. Cutin synthase abundance is the sum of transcripts mapping to several *G. raimondii* orthologs (as seen in Table 2, cotton often appears to have more copies encoding each protein than has *Arabidopsis* even though conservative approach has been adopted, i.e. sequences where annotations may be questioned have been left out). Orthology is not proof of conservation of function and neofunctionalisation of one or more orthologs cannot be ruled out but the error is deemed to be small.

KOR steadily increases as cell expansion progresses while cutin synthase declines as does expression of the transcription factors.

Judging from transcript levels, Fig. 2, where cutin synthase and the transcription factors that induce cutin synthesis follow similar trends, cutin synthesis appears to correlate inversely with cellulose deposition. This would lead to “dilution” of the cuticle as the fibre surface area increases, eventually allowing fibre fusion and deposition of the middle lamella. Cutin synthase is a GDSL-type lipase catalysing esterification in

the cuticle. The cutinase also belongs to the GDSL family but instead catalyses hydrolysis in the aqueous environment of the apoplast, for more information see the discussion in Fich et al. (2016).

It is worth noting that the expression profiles of the two diploid lines, 30834 and JWF15, are distinct from the profiles of the tetraploid lines in several cases.

Xyloglucan biosynthesis and deposition

Xyloglucan is a constituent of the middle lamella (Singh et al. 2009) and there it cannot hydrogen bond to cellulose and thus does not require strong base for extraction. Xyloglucan content declines steadily, and it is remarkably extractable in CDTA (Fig. 3). It should be noted here that anti-xyloglucan antibodies, and in particular LM25, are very high-affinity antibodies capable of detecting very small amounts. The ease of extraction is taken to reflect the localisation of the epitopes to the CFMLs. Cotton line JWF15 displayed a steeper rise in KOR expression between day 10 and 15, and a steeper decline in both cutin synthase and tightly bound xyloglucan in the same period corroborating the notion that these are tightly regulated processes.

Transcripts were not detected for all xyloglucan related GTs in all cotton lines. High level expression in early phases dominated by cell expansion of primary cell wall biosynthesis and CFML formation correlate generally with CoMPP data except for transcripts mapping to XXT2. The accumulation of xyloglucan in the CFML bulges preceding transitional phase as observed by Hernandez-Gomez et al. (2017) is not likely to be the result of *de novo* deposition given the profiles shown in Fig. 4. Rather, we propose an interpretation on terms of xyloglucan being depolymerised more slowly than other components of the bulges and thus being demasked for immunohistochemical detection.

RG-I biosynthesis and deposition

Pectin is a main constituent of middle lamellae, and also the point of attachment for the cuticle (Fich et al. 2016). Side-chains of RG-I are of particular interest given the metabolism of arabinan observed by Hernandez-Gomez et al. (2017) at around the time of onset of secondary wall deposition.

Three species were selected for immunohistochemistry of RG-I arabinan side-chains. Cell adhesion is not fully completed at 5 DPA in any of the varieties. Cell adhesion is complete and the bulges have disappeared at 17 DPA in JWF15 and FM966. Both galactan and arabinan accumulate early in fibre development in all species but the depolymerisation did not appear to follow the same kinetics in the three species, nor did the labeling display the same patterning at around the time of transition, when comparing 17 DPA micrographs in Fig. 5. The kinetics was further explored using CoMPP (Fig. 6). JWF15 appears to be developmentally ahead of in particular PimaS7 in agreement with the micrographs in Fig. 5 and with regard to up-regulation of KOR expression and down-regulation of genes involved in cutin biosynthesis. Correlation is observed in the NaOH extracts between INRA-RU2 (backbone), LM6 (branched arabinan), LM5 (galactan side-chains), but not with LM13 (linear arabinan). The highest amounts of CDTA-extractable LM6 epitope were observed at the earliest time point for all varieties with a tendency of LM13 peaking later in development. This is on the borderline of the resolution of the analysis but would corroborate the notion of the LM13 epitope being a product of arabinan debranching rather than synthesis *de novo*. The LM13 labeling of fibres at 25 DPA is very low, close to the detection limit (data not shown).

The INRA-RU2 probe detects unbranched and sparsely branched RG-I backbone. The CDTA profile of INRA-RU2 suggests general metabolism of RG-I side-chains thus creating more INRA-RU2 binding sites in this fraction. The quite different profile of INRA-RU2 binding to the NaOH extract may be rationalised if the RG-I backbone not extracted by CDTA was bound to cellulose via its side-chains (Zykwinska et al. 2005)

or via both side-chains and backbone (Larsen et al. 2011) thus requiring NaOH for extraction (Fig. 6).

Strict correlation between RG-I side-chains detected in the walls and the expression levels of the relevant GTs cannot be expected in light of the indications of side-chain metabolism. However, expression of GalS, the galactosyltransferase involved in RG-I galactan side-chain biosynthesis (Liwanag et al. 2012), correlates with the profile observed with LM5 in CoMPP with FM966 being the least expressed and 30834 being the highest. However, the delayed decline of the LM5 epitope in PimaS7 is not mirrored in its GalS-expression. It is not known whether the ARAD-genes are involved in either linear, branched or both kinds of arabinan hairs in RG-I (Harholt et al. 2012), and with the possible exception of 30384 it was not observed to be differentially expressed between species (Fig. 7).

RG-I side-chain metabolism

The plant cell secretome comprises a rich set of polysaccharide hydrolases suggesting that the cell wall is constantly being remodeled during development (Minic et al. 2007). Candidate enzymes for contributing to arabinan side-chain degradation are found in CAZy family GH3, to which both cotton and Arabidopsis have several genes assigned, and in family GH51, where two Arabidopsis genes are found and where we identified just a single *G. raimondii* gene. No cotton genes are classified to family GH51 at present. These enzymes are often annotated as bifunctional xylosidases/arabinofuranosidases but the activities have only been characterised in a few cases. Characterisation of an enzyme as having arabinofuranosidase activity does not suffice for assigning a role to the enzyme in RG-I catabolism. Although the degree of arabinose substitution of cotton xylan is expected to be low, if present, it could be a potential substrate for these enzymes. In addition, cotton, which is a dicot species, also has glycans on hydroxyproline-rich glycoproteins that could also act as substrate. Mutant studies have been used successfully to demonstrate that arabinan is the endogenous substrate of some GH3s in Arabidopsis (Minic et al. 2006; Arsovski et al. 2009). The GH51 enzyme appears to be a clear-cut arabinofuranosidase that acts on both pectic arabinan and on xylan while playing a role in secondary wall deposition in Arabidopsis (Montes et al. 2008; Ichinose et al. 2010).

The expression profiles of the putative arabinofuranosidase include some very highly expressed genes (Fig. 8). JFW15 is ahead of PimaS7 with regard to the most highly expressed GH3 but not ahead of 30384. The expression profiles of the individual GH3s are very different, suggesting involvement in different processes. The profiles of GH51 and the most highly expressed GH3 separate the diploids from the tetraploids possibly pointing to a role in fibre development.

Cell wall metabolism during fibre development has not been widely studied at the biochemical level in cotton. Transcripts encoding xyloglucan endotransglycosylases and expansins indicative of, in particular, xyloglucan remodelling are often observed in transcriptomic studies of fibre development, see Hande et al. (2017) for a recent example, but biochemical evidence for cell wall metabolism is presented less frequently. Implicating the hydrolases of Fig. 8 in fibre development requires that the wall turnover and relevant activities can be detected. Arabinofuranosidase activity was detected in freshly harvested fibres particularly in a fraction requiring high salt for extraction suggestive of localisation to the cell wall. The activity is very low (Fig. 9a). Given that enzyme extractability could be limiting, in muro autolysis was investigated by allowing fibres to digest in acetate buffer pH 5.5 overnight. Glucose release could be a result of callose turn-over but also starch is metabolised in fibres (e.g. Tang et al. 2017) and could contribute to the substantial glucose release. The release of other monosaccharides is generally low, (Fig. 9b). Xylose and galacturonic acid release are particularly low, making xylan, xyloglucan and homogalacturonan metabolism barely detectable. Fucose forms the non-reducing end of the F-chain of xyloglucan and since

this side-chain comprises a xylosyl residue as well it may be estimated that at most 20% of the fucose could originate from xyloglucan. The remainder of the fucose plus glucuronic acid both point to turnover of arabinogalactan protein (AGP). Rhamnose, arabinose and galactose are found in both RG-I and AGPs. The very low levels of activity prevent a detailed characterisation of the LiCl-extract of Fig. 9a but arabinose was released from a pure arabinan oligomer and arabinose and/or galactose was released from both RG-I and AGP-type substrates (Fig. 9c).

Discussion

Cotton quality relates to cell wall properties, such as compression and pulling strength and length of the cotton fibre, as well as more agronomical characteristics, such as the amount of leaf debris in the cotton. Intensive breeding for superior quality has greatly enhanced the strength and length of cotton fibres, especially with *G. barbadense* varieties. The existence of several species of relevance to cotton breeding with both diploid and tetraploid being important is both a complication and offers opportunities to map quality traits (Ademe et al, 2017). Fibre quality is variable among tetraploids but terapolidy is generally associated with long fibres and superior strength and fineness (Mishra et al. 2018). Parallel to classical breeding efforts, research into the correlation between cell wall biosynthesis/remodeling and cotton quality have let to insights in the main CESAs involved in primary and secondary cell wall cellulose biosynthesis, as well as the transcriptional regulation of primary and secondary cell wall biosynthesis and remodeling (Yuan et al. 2015; Hande et al. 2017)

It is reasonable to assume that fibre properties, length included, would be influenced by the primary cell wall, which acts as a scaffold for secondary wall deposition, as well as by the timing of the transition from primary to secondary wall biosynthesis. While the cotton species and varieties studied here did not develop in perfect synchrony, the transition was remarkably consistent using the peak in easily extractable callose as a marker of the transition (Fig.1). However, early developmental events differed greatly in particular among varieties as demonstrated in the studies of the CFML by Hernandez-Gomez et al. (2017). The observed cell wall metabolic processes are incompletely understood at present, and it is not altogether clear which processes contribute to adhesion and which to detachment. It was the object of the present study to gain insight into the cell wall metabolism during the early period where fibres fuse.

Postgenital fusion

Epidermal walls are normally coated with a cuticle and only when it is absent may organ fusion occur including formation of a new middle lamella that does not originate from a phragmoplast. The data presented here on the expression of genes involved in cutin biosynthesis supports a view that cotton fibre fusion and CFML formation depends on cutin dilution as being a result of cell elongation while cutin synthesis has ceased thus permitting fusion shortly after fibre emergence from the epidermis. Cutinase expression followed a similar trend as that of the cutin synthase. A note of caution is in order here. Both cutin synthase and cutinase are lipases and Fich et al. (2016) pointed out that whether these enzymes catalyse hydrolysis or esterification depends on the environment being aqueous or more hydrophobic. Comparing the abundance of transcripts, in FM966 for example, mapping to the cutin synthase and cutinase respectively (Fig. 2) may lead to the hypothesis that FM966 hardly synthesises cutin unless the cutinase is indeed used as a synthase. CUS1 in *Arabidopsis* is co-expressed with several GDSL-type lipases (ATTED-II, <http://atted.jp>, data not shown) most of which belong to the same clade as CUS1. Co-expression is also observed with GDSL lipase AtLPEAT2 annotated as an acyltransferase (Stahlberg et al. 2009) but not with lipases annotated as hydrolases nor with CDEF1,

the gene used here for the selection of putative *G. raimondii* cutinases. Nevertheless, the decline in cutin synthase expression, with or without adding a contribution from the transcripts annotated as cutinases, combined with the rapid fibre elongation support the notion of a dramatic dilution of cutin so that no degradation is required to allow fusion. Mature cotton fibres are not devoid of cutin and cutin biosynthetic genes have been found to be upregulated later in fibre development (Tuttle et al. 2015). Hence, the dip in cutin biosynthesis is transitory.

Xyloglucan

Hemicelluloses were originally defined by their extractability by strong alkali but hardly by milder solvents, but several exceptions to this rule has led to adoption of a definition defined by structure (Scheller and Ulvskov 2010). Xyloglucan located in the CFML, where it does not associate with cellulose and thus is CDTA extractable, is but an extra example already observed by Avci et al. (2013). These authors found *G. barbadense* and *hirsutum* to differ radically in that loosely bound xyloglucan was nearly absent in *G. barbadense*. We observed the expression of *ClcC4* to be low or rapidly declining in all varieties in agreement with the observations by Tuttle et al. (2015) and MacMillan et al. (2017). *MUR3* and *CslC4* were quite lowly expressed in *G. barbadense* PimaS7 but the CoMPP analyses did not indicate absence of CDTA-extractable xyloglucan in PimaS7. The CoMPP-data suggests that this xyloglucan population existed from CFML deposition onwards and that its detection by Hernandez-Gomez et al. (2017), in particular during CFML metabolism, is most likely a result of improved antibody accessibility. CDTA extractable xyloglucan declines sharply while the NaOH extractable xyloglucan declines more slowly. The thicker, cellulose enriched secondary walls of the more mature fibres will lead to relatively lower signals for tightly bound xyloglucan even in the absence of degradation or reduced extractability in the more mature fibres. GTs involved in xyloglucan side-chain biosynthesis are often observed to be very lowly expressed in growing cells as well. The declining expression of the *CslC4* (backbone synthesis) and the very low expression of the side-chain synthesising GTs suggests that the tightly bound xyloglucan that persists is not turned over; only the CDTA-extractable xyloglucan appears to be metabolised.

RG-I

Sørensen et al. (2000) observed that the LM5 epitope (β -1,4-galactan) was most abundant near the plasma membrane. This may be interpreted in favor of different populations of RG-I or as metabolism as tiles in the wall moved outward during cell expansion (Ulvskov et al. 2005). Development of a new RG-I probe led to clear indications of a different RG-I species located at the middle lamella (Buffetto et al. 2015). Also, there are examples of masking of RG-I epitopes as well as indications of different RG-I epitopes being detected in different regions of cell walls in relation to middle lamellae (Lee et al. 2013). It is safe to conclude that we have more than one kind of RG-I in the developing cotton fibre. Whether more than one kind are synthesised de novo, or if they are the result of metabolism, we cannot tell and the two possibilities are not mutually exclusive. The LM6 and the LM13 epitopes clearly display separate profiles as would be expected. We propose that arabinan degradation is a prerequisite for formation of a middle lamella suited to later dissolution and cell separation and infer this on the basis of the high levels of hydrolase expression at around the time CFML completion. Full detachment is achieved substantially later, and is assumed to involve a complete disassembly of the CFML. It remains a conundrum that the measured hydrolase activities were so low. It might be hypothesised that arabinofuranosidases are auxiliary enzymes to a cotton endo-arabinanase. There is very little to go on with regard to identifying the endo-arabinanase(s). This activity is not known from plants and is therefore entirely hypothetical. It may be speculated that

it is to be found in family GH43 but to-date no plant enzyme from this family has been biochemically characterised.

Perspectives

Transition to secondary wall deposition in cotton fibre is accompanied by a complex set of wall metabolic processes leading to CFML dissolution and fibre detachment. Used as an experimental system it may be instrumental in elucidating which families of hydrolases take part in RG-I metabolism not only in cotton. These observations also serve as cautionary note in case time of transition is seen as a breeding target for improved fibre properties. The complexity of the transition process suggests that it should be modulated via an upstream factor rather than through expression of genes encoding enzymes directly involved in wall metabolism in cotton fibre at the time of transition.

References

Ademe MS, He S, Pan Z, Sun J, Wang Q, Qin H, Liu J, Liu H, Yang J, Xu D, Yang J, Ma Z, Zhang J, Li Z, Cai Z, Zhang X, Zhang X, Huang A, Yi X, Zhou G, Li L, Zhu H, Pang B, Wang L, Jia Y, Du X (2017) Association mapping analysis of fiber yield and quality traits in upland cotton (*Gossypium hirsutum* L.). *Mol Genet Genomics* 292:1267-1280. doi: 10.1007/s00438-017-1346-9.

Arsovski AA, Popma TM, Haughn GW, Carpita NC, McCann MC, Western TL (2009) AtBXL1 encodes a bifunctional β -D-xylosidase/ α -L-arabinofuranosidase required for pectic arabinan modification in *Arabidopsis* mucilage secretory cells. *Plant Physiol* 150:1219-1234

Avci U, Pattathil S, Singh B, Brown VL, Hahn MG, Haigler CH (2013) Cotton fiber cell walls of *Gossypium hirsutum* and *Gossypium barbadense* have differences related to loosely-bound xyloglucan. *Plos One* 8: article e56315

Buffetto F, Cornuault V, Rydahl MG, Ropartz D, Alvarado C, Echasserieau V, Le Gall S, Bouchet B, Tranquet O, Verherbruggen Y, Willats WGT, Knox JP, Ralet MC, Guillon F (2015) The deconstruction of pectic rhamnogalacturonan I unmasks the occurrence of a novel arabinogalactan oligosaccharide epitope. *Plant Cell Physiol* 56:2181-2196

Byg I, Diaz J, Øgden LH, Harholt J, Jørgensen B, Rolin C, Svava R, Ulvskov P (2012) Large-scale extraction of rhamnogalacturonan I from industrial potato waste. *Food Chem* 131: 07–1216

Fich EA, Segerson NA, Rose JCK (2016) The plant polyester cutin: biosynthesis, structure, and biological roles. *Annu Rev Plant Biol* 67:207-233

Haigler CH, Betancur L, Stiff MR, Tuttle JR (2012) Cotton fiber: a powerful single-cell model for cell wall and cellulose research. *Front Plant Sci* 3: DOI:10.3389/fpls.2012.00104

Hande AS, Katageri IS, Jadhav MP, Adiger S, Gamanagatti S, Padmalatha KV, Dhandapani G, Kanakachari M, Kumar PA, Reddy VS (2017) Transcript profiling of genes expressed during fibre development in diploid cotton (*Gossypium arboreum* L.). *BMC Genomics* 18: article 675 DOI: 10.1186/s12864-017-4066-y

Harholt J, Jensen JK, Verherbruggen Y, Sogaard C, Bernard S, Nafisi M, Poulsen CP, Geshi N, Sakuragi, Driouch A, Knox JP, Scheller HV (2012) ARAD proteins associated with pectic arabinan biosynthesis form complexes when transiently overexpressed in planta. *Planta* 236:115-128

Hernandez-Gomez MC, Runavot JL, Guo XY, Bourot S, Benians TAS, Willats WGT, Meulewaeter F, Knox JP (2015a) Heteromannan and heteroxylan cell wall polysaccharides display different dynamics during the elongation and secondary cell

wall deposition phases of cotton fiber cell development. *Plant Cell Physiol* 56:1786-1797

Hernandez-Gomez MC, Runavot JL, Meulewaeter F, Knox JP (2017) Developmental features of cotton fibre middle lamellae in relation to cell adhesion and cell detachment in cultivars with distinct fibre qualities. *BMC Plant Biol* 17:69 doi: 10.1186/s12870-017-1017-3

Hernandez-Gomez MC, Rydahl MG, Rogowski A, Morland C, Cartmell A, Crouch L, Labourel A, Fontes CMGA, Willats WGT, Gilbert HJ, Knox, JP (2015b) Recognition of xyloglucan by the crystalline cellulose-binding site of a family 3a carbohydrate-binding module. *FEBS Lett* 589:2297-2303

Ichinose H, Nishikubo N, Demura T, Kaneko S (2010) Characterization of α -L-arabinofuranosidase related to the secondary cell walls formation in *Arabidopsis thaliana*. *Plant Biotechnol* 27:259-266

Iwai H, Ishii T, Satoh S (2001) Absence of arabinan in the side chains of the pectic polysaccharides strongly associated with cell walls of *Nicotiana plumbaginifolia* non-organogenic callus with loosely attached constituent cells. *Planta* 213:907-915

Jarvis MC, Briggs SPH, Knox JP (2003) Intercellular adhesion and cell separation in plants. *Plant Cell Environ* 26:977–989

Jones L, Seymour GB, Knox JP (1997) Localization of pectic galactan in tomato cell walls using a monoclonal antibody specific to (1→4)- β -D-galactan. *Plant Physiol* 113:1405-1412

Kim HJ, Triplett BA (2001) Cotton fiber growth in planta and in vitro. Models for plant cell elongation and cell wall biogenesis. *Plant Physiol* 127:1361-1366

Kljun A, El-Dessouky HM, Benians TAS, Goubet F, Meulewaeter F, Knox JP, Blackburn JS (2014) Analysis of the physical properties of developing cotton fibres. *Eur Polym J* 51:57–68

Larsen FH, Byg I, Diaz J, Engelsen SB, Ulvskov P (2011) Residue specific hydration of primary cell wall potato pectin identified by solid-state ^{13}C single-pulse MAS and CP/MAS NMR spectroscopy. *Biomacromolecules* 12:1844-1850

Lee KJD, Cornuault V, Manfield I, Ralet M-C, Knox JP (2013) Multiscale spatial heterogeneity of pectic rhamnogalacturonan-I (RG-I) in tobacco seed endosperm cell walls. *Plant J* 75:1018–1027

Li Z, Fernie AR, Persson S (2016) Transition of primary to secondary cell wall synthesis. *Sci Bull* 61:838-846

Liwanag AJM, Ebert B, Verhertbruggen Y, Rennie EA, Rautengarten C, Oikawa A, Andersen MCF, Clausen MH, Scheller HV (2012) Pectin biosynthesis: GALS1 in *Arabidopsis thaliana* is a β -1,4-galactan β -1,4-galactosyltransferase. *Plant Cell* 24:5024-5036

MacMillan CP, Birke H, Chuah A, Brill E, Tsuji Y, Ralph J, Dennis ES, Llewellyn D, Pettolino FA (2017) Tissue and cell-specific transcriptomes in cotton reveal the subtleties of gene regulation underlying the diversity of plant secondary walls. *BMC Genomics* 18: article 539

Maltby D, Carpita NC, Montezinos D, Kulow C, Delmer DP (1979) β -1,3-glucan in developing cotton fibers - structure, localization, and relationship of synthesis to that of secondary wall cellulose. *Plant Physiol* 63:1158-1164

Marcus SE, Verhertbruggen Y, Hervé C, Ordaz-Ortiz JJ, Farkas V, Pedersen HL, Willats WG, Knox JP (2008) Pectic homogalacturonan masks abundant sets of xyloglucan epitopes in plant cell walls. *BMC Plant Biol*. 8:60. doi: 10.1186/1471-2229-8-60

McCann M, Roberts K (1994) Changes in cell wall architecture during cell elongation. *J Exp Bot* 45:1683-1691

- Meikle PJ, Bonig I, Hoogenraad NJ, Clarke AE, Stone BA (1991) The location of (1→3)- β -glucans in the walls of pollen tubes of *Nicotiana glauca* using a (1→3)- β -glucan-specific monoclonal antibody. *Planta* 185:1–8
- Michailidis G, Argiriou A, Darzentas N, Tsaftaris A (2009) Analysis of xyloglucan endotransglycosylase/hydrolase (XTH) genes from allotetraploid (*Gossypium hirsutum*) cotton and its diploid progenitors expressed during fiber elongation. *J Plant Physiol* 166:403-416.
- Minic Z, Do CT, Rihouey C, Morin H, Lerouge P, Jouanin L (2006) Purification, functional characterization, cloning, and identification of mutants of a seed-specific arabinan hydrolase in *Arabidopsis*. *J Exp Bot* 57:2339-2351
- Minic Z, Jamet E, Negroni L, der Garabedian PA, Zivy M, Jouanin L (2007) A sub-proteome of *Arabidopsis thaliana* mature stems trapped on concanavalin A is enriched in cell wall glycoside hydrolases. *J Exp Bot* 58:2503-2512
- Mishra DK, Agrawa N, Choudhary A, Yadav VK, Yadav VK (2018) An overview on advances in cotton genome and regulation of fiber development. *ISJR* 7:294-300
- Molhoj M, Johansen B, Ulvskov P, Borkhardt B (2001) Expression of a membrane-anchored endo-1,4- β -glucanase from *Brassica napus*, orthologous to KOR from *Arabidopsis thaliana*, is inversely correlated to elongation in light-grown plants. *Plant Mol Biol* 45:93-105
- Moller I, Marcus SE, Haeger A, Verhertbruggen Y, Verhoef R, Schols H, Ulvskov P, Mikkelsen JD, Knox JP, Willats W. (2008) High-throughput screening of monoclonal antibodies against plant cell wall glycans by hierarchical clustering of their carbohydrate microarray binding profiles. *Glycoconj J* 25:37-48
- Montes RAC, Ranocha P, Martinez Y, Minic Z, Jouanin L, Marquis M, Saulnier L, Fulton LM, Cobbett CS, Bitton F, Renou JP, Jauneau A, Goffner D (2008) Cell wall modifications in *Arabidopsis* plants with altered α -L-arabinofuranosidase activity. *Plant Physiol* 147:63-77
- Nicol F, His I, Jauneau A, Vernhettes S, Canut H, Höfte H (1998) A plasma membrane-bound putative endo-1,4- β -D-glucanase is required for normal wall assembly and cell elongation in *Arabidopsis*. *EMBO J* 17:5563-5576.
- Orford S J, Timmis JN (1998). Specific expression of an expansin gene during elongation of cotton fibres. *BBA-Gene Struct Expr* 1398:342-346.
- Pedersen HL, Fangel JU, McCleary B, Ruzanski C, Rydahl MG, Ralet MC, Farkas V, von Schantz L, Marcus SE, Andersen MC, Field R, Ohlin M, Knox JP, Clausen MH, Willats WG (2012) Versatile high resolution oligosaccharide microarrays for plant glycobiology and cell wall research. *J Biol Chem* 287:39429-39438. doi: 10.1074
- Qin LX, Rao Y, Li L, Huang JF, Xu WL, Li XB (2013) Cotton GalT1 encoding a putative glycosyltransferase is involved in regulation of cell wall pectin biosynthesis during plant development. *Plos ONE* 8: Article e59115 DOI:10.1371/journal.pone.0059115
- Ralet M-C, Tranquet O, Poulain D, Moise A, Guillon F. (2010) Monoclonal antibodies to rhamnogalacturonan I backbone. *Planta* 231:1373-1383
- Ruprecht C, Mutwil M, Saxe F, Eder M, Nikoloski Z, Persson S (2011) Large-scale co-expression approach to dissect secondary cell wall formation across plant species. *Front Plant Sci* DOI:10.3389/fpls.2011.00023
- Shao MY, Wang XD, Ni M, Bibi N, Yuan SN, Malik W, Zhang HP, Liu YX, Hua SJ (2011) Regulation of cotton fiber elongation by xyloglucan endotransglycosylase/hydrolase genes. *Genet Mol Res* 10:3771-3782.
- Shimizu Y, Aotsuka S, Hasegawa O, Kawada T, Sakuno T, Sakai F, Hayashi T (1997) Changes in levels of mRNAs for cell wall-related enzymes in growing cotton fiber cells. *Plant Cell Physiol* 38:375-378.
- Singh B, Avci U, Inwood SEE, Grimson MJ, Landgraf J, Mohnen D, Sorensen I, Wilkerson CG, Willats WGT, Haigler CH (2009) A specialized outer layer of the primary

cell wall joins elongating cotton fibers into tissue-like bundles. *Plant Physiol* 150:684-699

Stalberg K, Stahl U, Stymne S, Ohlrogge J (2009) Characterization of two *Arabidopsis thaliana* acyltransferases with preference for lysophosphatidylethanolamine. *BMC Plant Biol* 9: DOI: 10.1186/1471-2229-9-60

Sørensen SO, Pauly M, Bush M, Skjøt M, McCann MC, Borkhardt B, Ulvskov, P (2000) Pectin engineering: Modification of potato pectin by in vivo expression of an endo-1,4- β -D-galactanase. *P Natl Acad Sci USA* 97:7639–7644

Tang, F, Zhu J, Wang T, Shao D (2017) Water deficit effects on carbon metabolism in cotton fibers during fiber elongation phase. *Acta Physiol Plant* 39: article 69

Tuttle JR, Nah G, Duke MV, Alexander DC, Guan X, Song Q, Chen ZJ, Scheffler BE, Haigler CH (2015) Metabolic and transcriptomic insights into how cotton fiber transitions to secondary wall synthesis, represses lignification, and prolongs elongation. *BMC Genomics* 16: article 477

Ulvskov P, Wium, H, Bruce D, Jørgensen B, Bruun Qvist K, Skjøt M, Hepworth DM, Borkhardt B, Sørensen S (2005) Biophysical consequences of remodeling the neutral side chains of rhamnogalacturonan I in tubers of transgenic potatoes. *Planta* 220:609-620

van der Schoot C, Dietrich MA, Storms M, Verbeke JA, Lucas WJ (1995) Establishment of a cell-to-cell communication pathway between separate carpels during gynoecium development. *Planta* 195:450-455

Verbeke JA (1992) Fusion events during floral morphogenesis. *Ann Rev Plant Physio* 43:583–598

Willats WGT, Marcus SE, Knox JP (1998) Generation of a monoclonal antibody specific to (1 \rightarrow 5)- α -l-arabinan. *Carbohydr Res* 308: 49-152

Yang YW, Bian SM, Yao Y, Liu JY (2008) Comparative proteomic analysis provides new insights into the fiber elongating process in cotton. *Proteome Res* 7:4623–4637

Yuan D, Tang Z, Wang M, Gao W, Tu L, Jin X, Chen L, He Y, Zhang L, Zhu L, Li Y, Liang Q, Lin Z, Yang X, Liu N, Jin S, Lei Y, Ding Y, Li G, Ruan X, Ruan Y, Zhang X (2015) The genome sequence of Sea-Island cotton (*Gossypium barbadense*) provides insights into the allopolyploidization and development of superior spinnable fibres. *Nature Scientific Reports* 5, Article number: 17662 DOI:10.1038/srep17662

Zhong J, Preston JC (2015) Bridging the gaps: evolution and development of perianth fusion. *New Phytol* 208:330–335

Zhong RQ, Burk DH, Ye ZH (2011) Fibers. A model for studying cell differentiation, cell elongation, and cell wall biosynthesis. *Plant Physiol* 126:477-479

Zykwinska AW, Ralet MCJ, Garnier CD, Thibault JFJ (2005) Evidence for in vitro binding of pectin side chains to cellulose. *Plant Physiol* 139:397-407

Table 1 Antibody probes used in CoMPP and immunohistochemistry

Probe	Specificity	Reference
LM5	(1,4)- β -D-Gal ₄	Jones et al. (1997)
LM6	(1,5)- α -L-Araf ₅ , branches tolerated	Willats et al. (1998)
LM13	Longer, unbranched (1,5)- α -L-Araf _n	Moller et al. (2008)
INRA-RU2	Rha-(1,4)-GalA-(1,2)- Rha-(1,4)-GalA-(1,2)- of RG-I	Ralet et al. (2010)
LM15	XXXG-motif in xyloglucan	Marcus et al. (2008)
LM25	XLLG, XLG, XXXG in xyloglucan	Pedersen et al. (2012)
BS-400-2	(1,3)- β -D-glucan (callose)	Meikle et al. (1991)

Table 2 Orthology assignment of transcripts. The IDs are not cotton annotations but protein identifiers of the Arabidopsis orthologs used for assignment except for GH3 and GH51 which are glycosylhydrolase family identifiers. Entry 1 is related to cellulose synthesis; 2-6 cutin biosynthesis; 7 cutin degradation; 8-12 to xyloglucan biosynthesis; 13-14 to rhamnogalacturonan-I side-chain biosynthesis and 15-16 to arabinan degradation

#	ID	<i>G. raimondii</i> locus
1	Korrigan (KOR)	Gorai.010G143300
2	Cutin synthase (CUS1)	Gorai.004G249700 Gorai.004G249800 Gorai.001G235500 Gorai.007G271400 Gorai.007G271700 Gorai.013G119200 Gorai.013G119300 Gorai.013G188900
3	ANL2	Gorai.001G171000 Gorai.004G120700 Gorai.006G047300 Gorai.010G177800 Gorai.011G016200
4	HDG1	Gorai.007G096000, Gorai.013G100200
5	MYB16	Gorai.011G122800 Gorai.012G186500 Gorai.013G088300
6	MYB106	Gorai.012G052500
7	Cutinase (CDEF1)	Gorai.004G026600 Gorai.009G003600 Gorai.009G159200 Gorai.010G240200 Gorai.011G035400
8	CslC4	Gorai.006G028400
9	Fucosyltransferase (XG-FUT)	Gorai.013G088600
10	XG-XXT1	Gorai.005G060400
11	XG-XXT2	Gorai.007G128800
12	MUR3	Gorai.007G150100
13	GALS	Gorai.007G359700 Gorai.006G138000 Gorai.008G052100 Gorai.009G345800
14	ARAD	Gorai.008G052100 Gorai.007G359700 Gorai.006G138000 Gorai.009G345800
15	GH51	Gorai.002G225800
16	GH3	Gorai.005G218000 Gorai.006G259500 Gorai.001G143600 Gorai.011G198200

Figure legends

Fig. 1 CDTA- and NaOH-extractable callose in developing cotton fibres, as detected by antibody probe BS-400-2 in CoMPP. X-axis is days post anthesis (DPA) and Y-axis is CoMPP signal relative to the maximal signal on the array

Fig. 2 Transcripts of genes encoding enzymes and transcription factors involved in cutin metabolism as related to rate of secondary wall deposition for which Korrigan (KOR) is used as marker due to its involvement in cellulose deposition. CUS1 and CDEF1 are lipases involved in formation and hydrolysis of ester linkages in cutin. ANL2, HDG1, myb 16 and myb 106 are transcription factors. X-axis is days post anthesis, DPA, and Y-axis is relative expression (see Materials and Methods for an explanation of Y-axis scaling)

Fig. 3 Loosely and tightly bound xyloglucan. CDTA and NaOH extractable xyloglucan as detected by antibodies LM15 and LM25 (see the antibody table in Materials and Methods for details on the two probes). Axis labeling as in Fig. 1

Fig. 4 Transcript profiles of genes involved in xyloglucan biosynthesis, CSLC4 for the backbone synthase, FUT for the fucosyl transferase that generates F-chain, the XXTs that add xylose to the backbone glucan and MUR3 that transfers Gal to xylosyl side-chains thus generating the L-chain. Axis labeling as in Fig. 2

Fig. 5 Immunolocalization of the INRA-RU2 RG-I backbone epitope. Cross sections of developing and mature cotton fibres of PimaS7 (*G. barbadense*), FM966 (*G. hirsutum*) and JFW15 (*G. arboreum*). The RG-I backbone epitope was abundant in the fibre primary cell wall of all cultivars at all timepoints. RG-I backbone degradation was mainly detected in the JFW15 line (arrowheads). Also, the FM966 and PimaS7 lines showed similar signs of degradation only at 25 dpa. Scale bar: 10 μ m.

Fig. 6 Cross sections of developing cotton fibres of PimaS7 (*G. barbadense*), FM966 (*G. hirsutum*) and JFW15 (*G. arboreum*) immunolabeled for RG-I side chain arabinan. LM6: branched arabinan epitope. The LM6 arabinan epitope was found intracellularly LM6 (arrow in FM966 5 DPA and PimaS7 17 DPA panels) and was part of the CFML (arrowhead in the JFW15 5 DPA panel). LM13: linear arabinan epitope. While the arabinan LM6 epitope bound to the particles of the CFML the LM13 linear arabinan epitope did not (arrowheads). A zone of stronger labelling between neighbouring cell walls was observed at 17 DPA in FM966 and JFW15 (arrows). Scale bars: 10 μ m

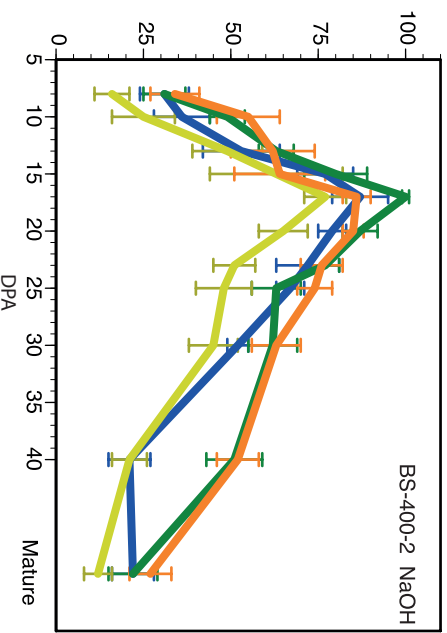
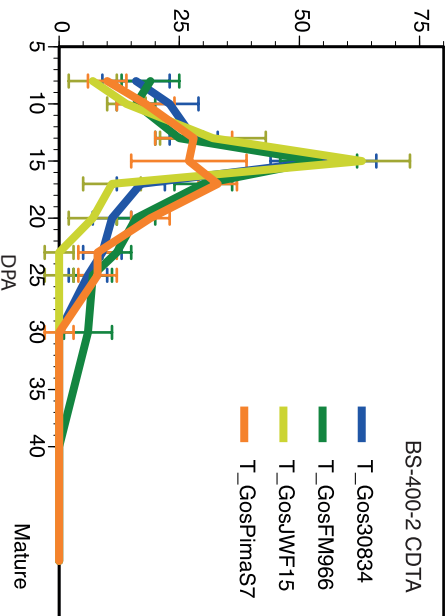
Fig. 7 CoMPP of RG-I epitopes comprising galactan side-chains (LM5), branched arabinan side-chains (LM6), linear arabinan side-chains (LM13) and RG-I backbone (INRA-RU2)

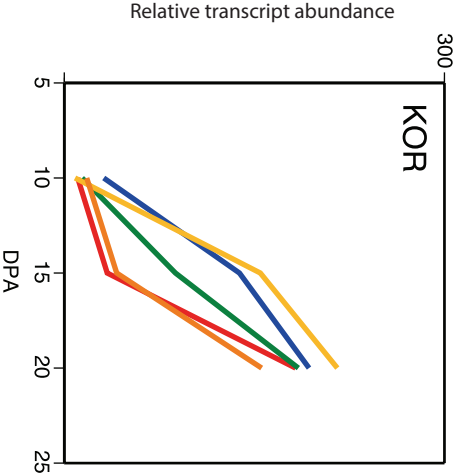
Fig. 8 RG-I side-chain biosynthesis. Expression profiles for GalS, the β -galactan galactosyltransferase of GT92, and transcripts mapping to ARAD, the putative arabinosyltransferases of family GT47

Fig. 9 Enzyme activities potentially contributing to RG-I side-chain degradation. Transcriptomic profiling of putative arabinofuranosidases in the five cotton lines

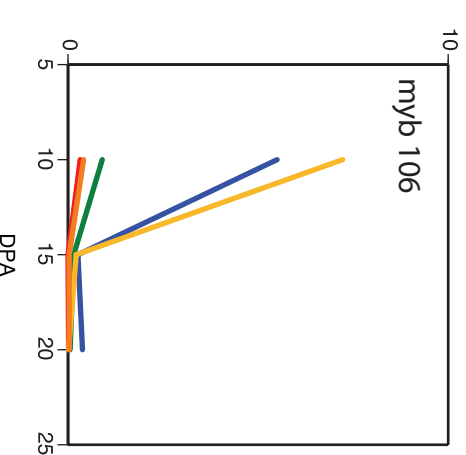
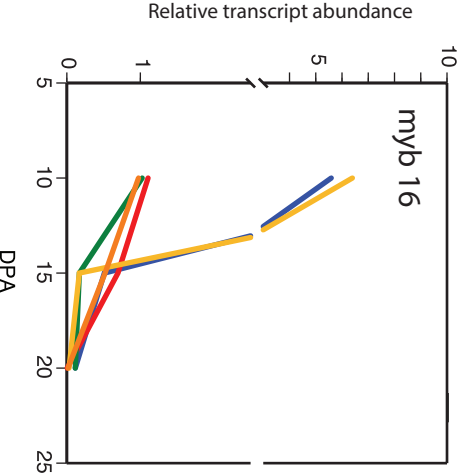
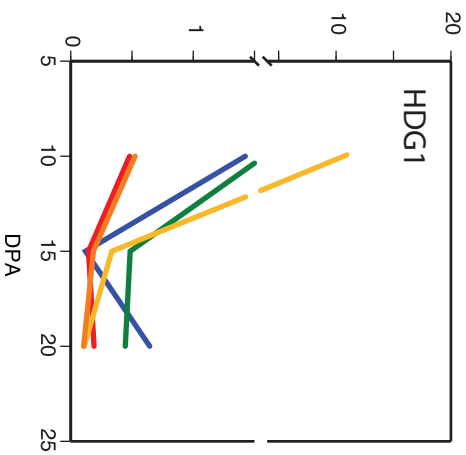
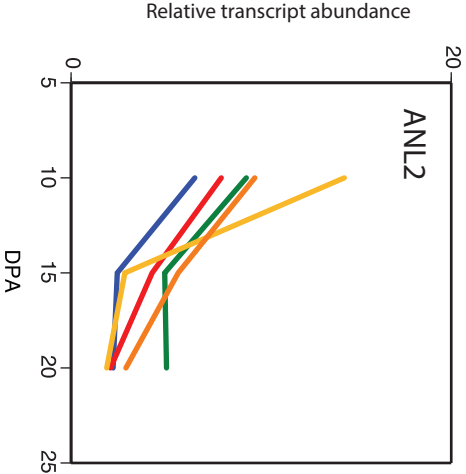
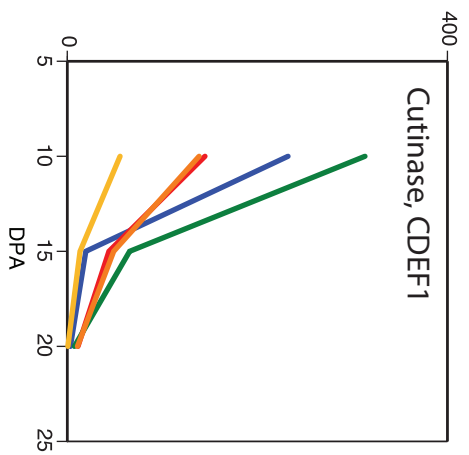
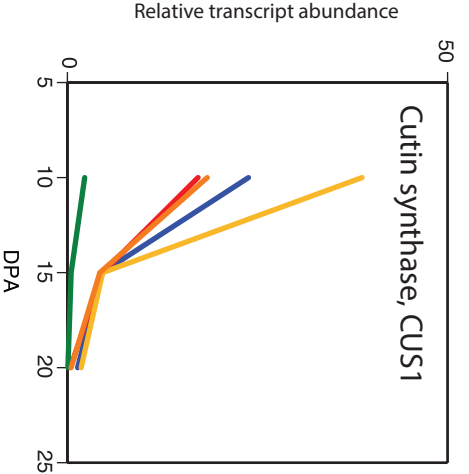
Fig. 10 Polysaccharide hydrolase activities and fibre wall autolysis. **a** release of p-nitrophenyl from p-nitrophenyl- β -arabinofuranoside by locular sap and fibre extracts. **b** monosaccharide profiles of two over-night autodigests. **c** release of arabinose plus galactose from selected RG-I and AGP substrates by the LiCl-extract of panel **a**

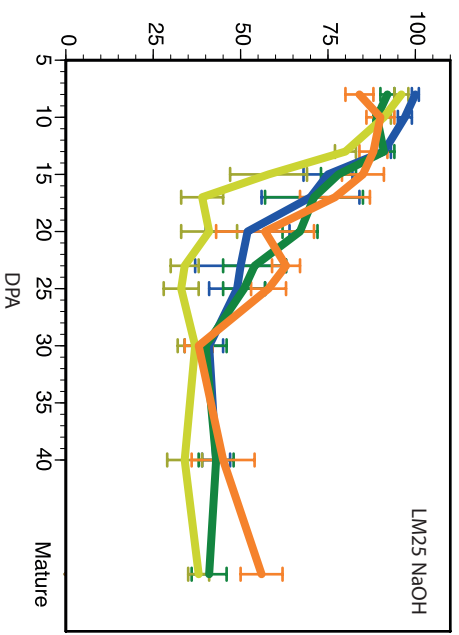
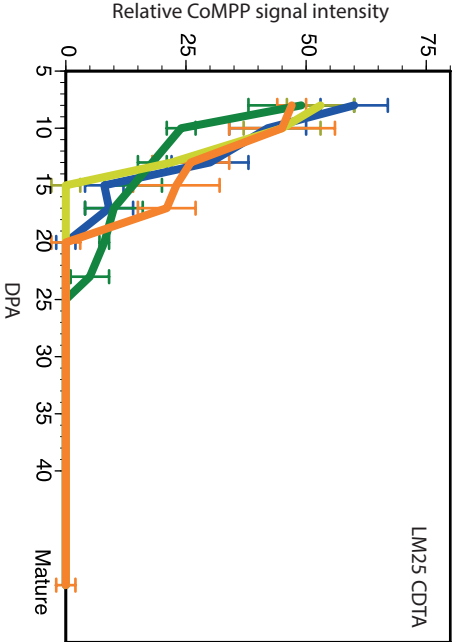
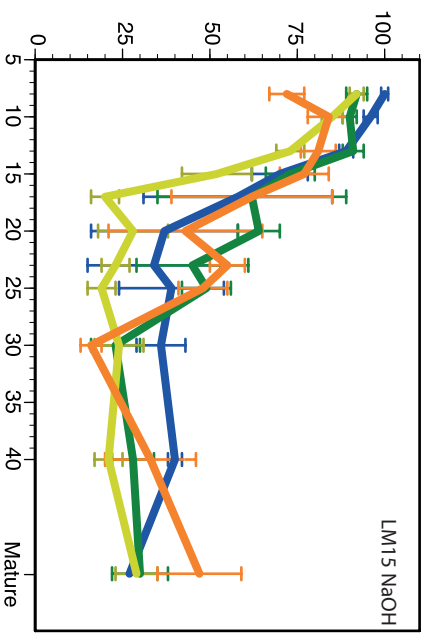
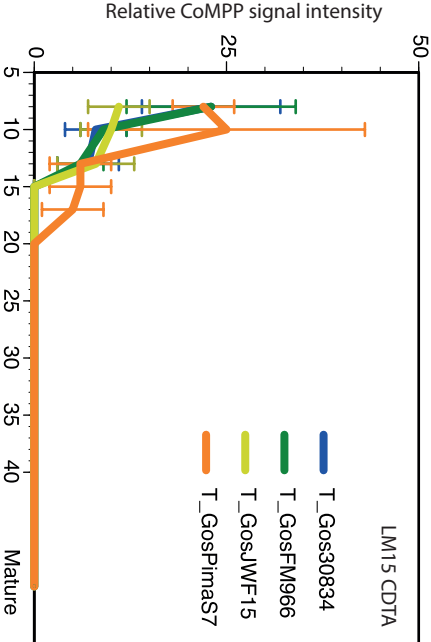
Relative CoMPP signal intensity

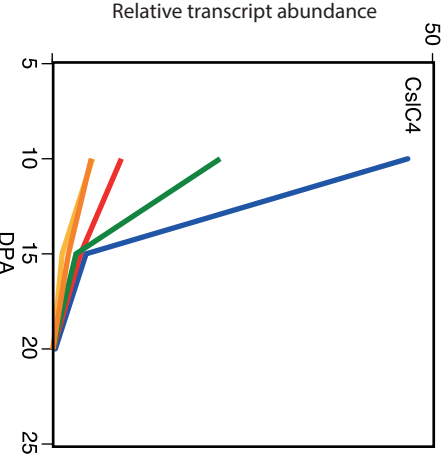




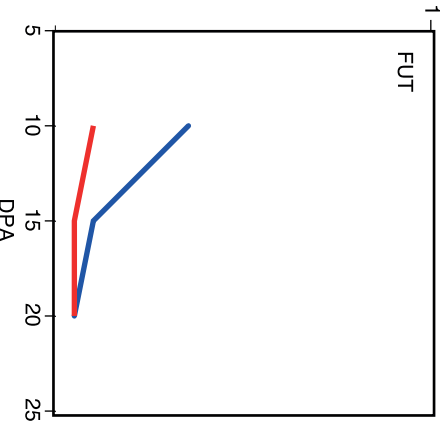
T_Gos30834
T_GosChina10
T_GosFM966
T_GosJFW15
T_GosPimas7



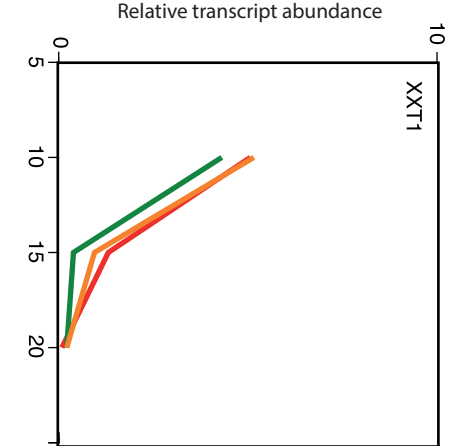




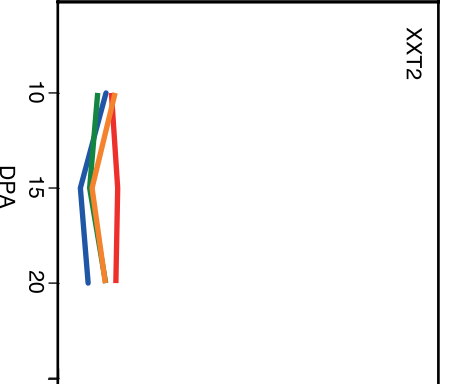
T_Gos30834
 T_GosChina
 T_GosFM966
 T_GosJFW15
 T_GosPimaS7



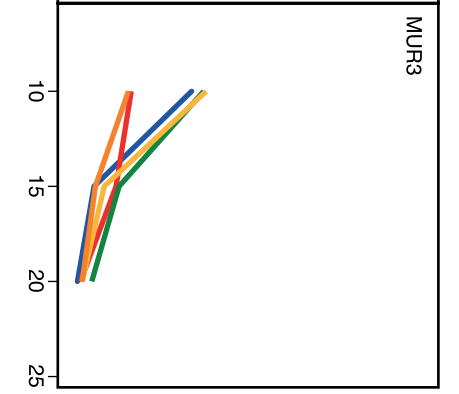
FUT



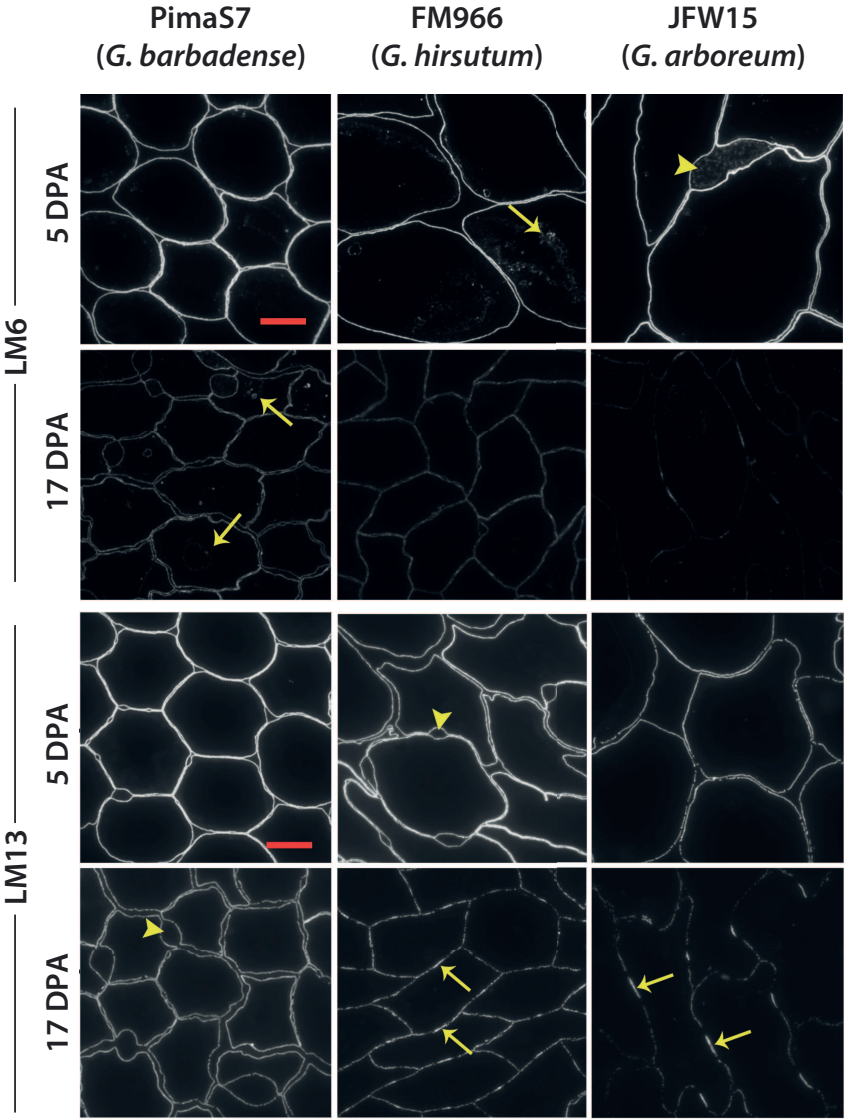
XXT1

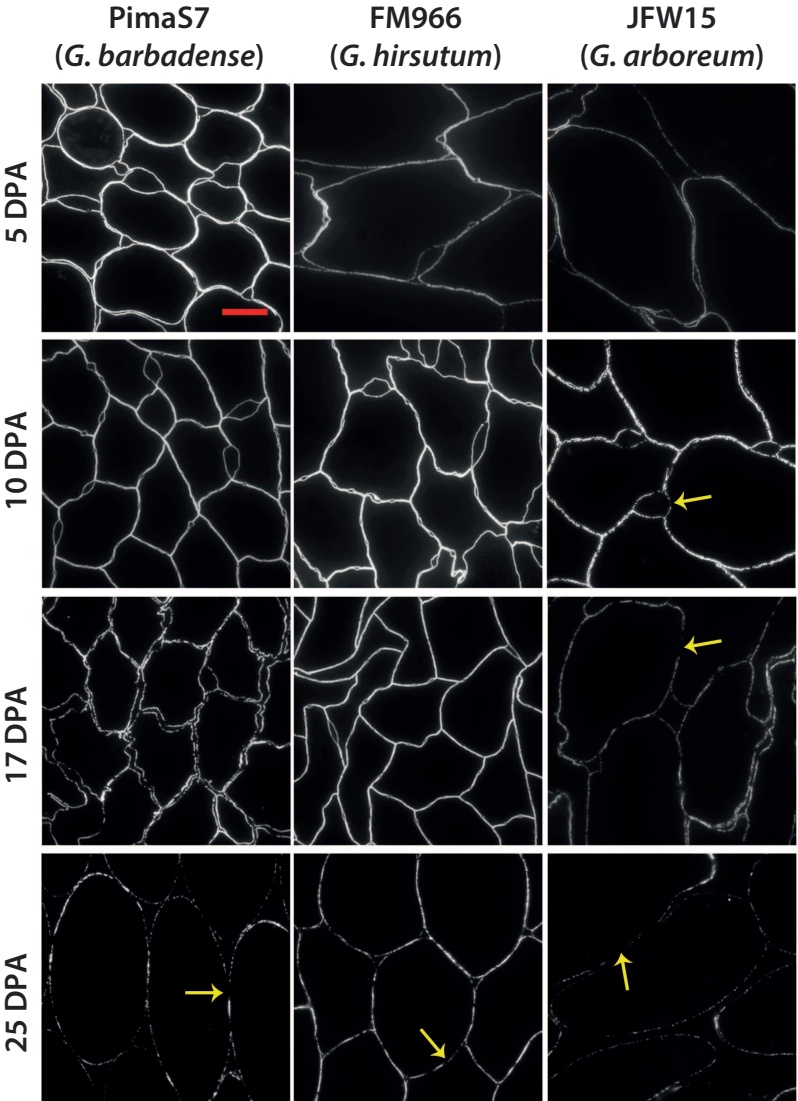


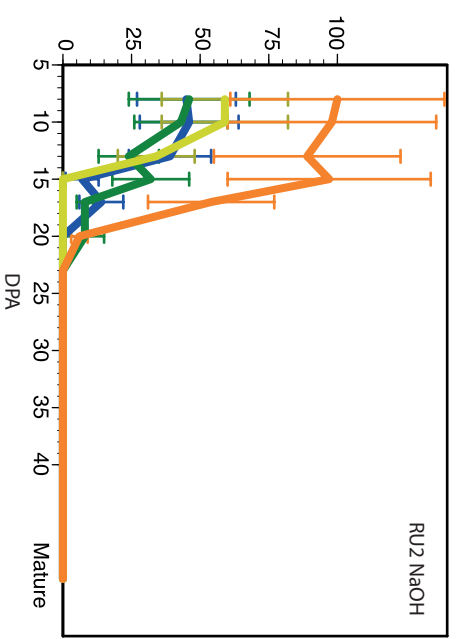
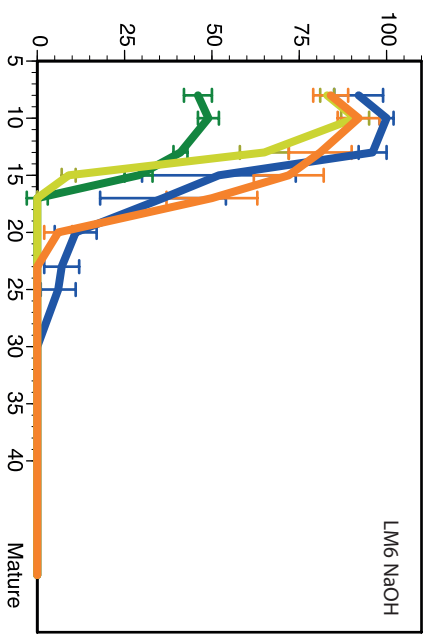
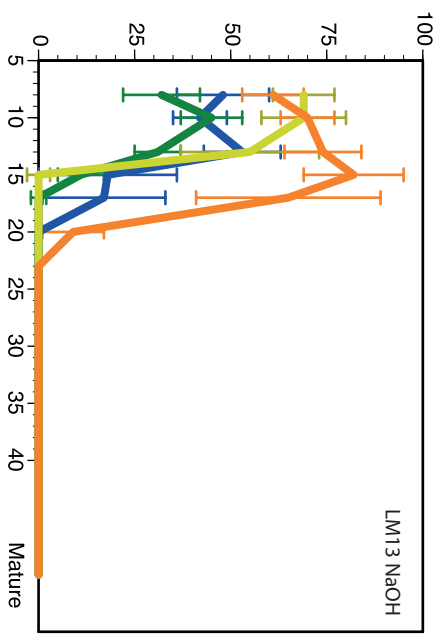
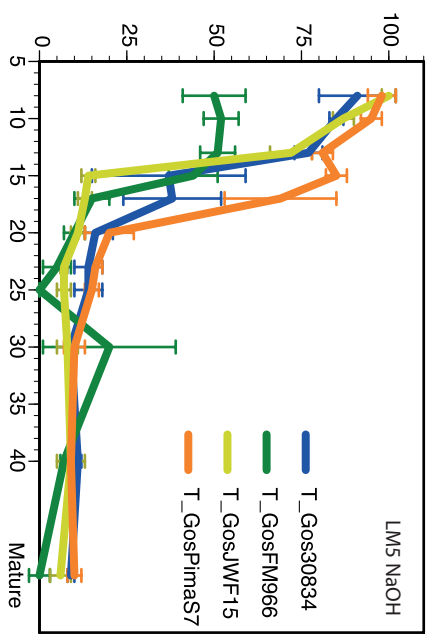
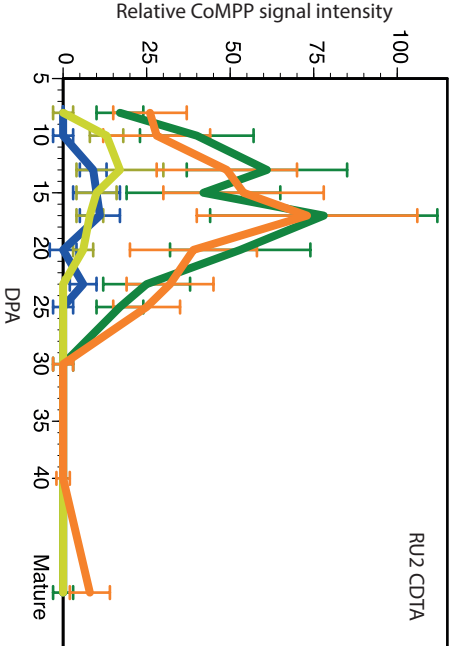
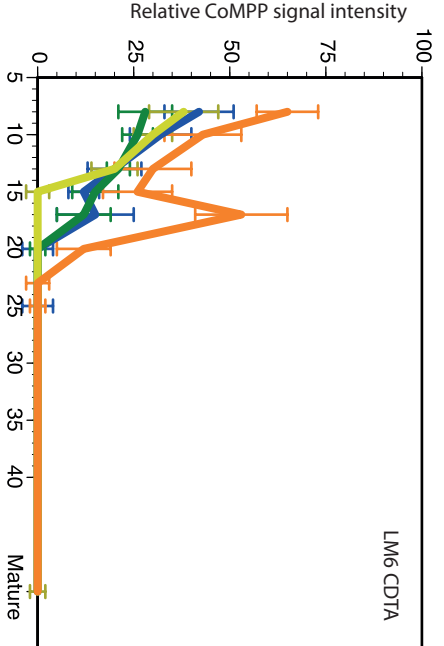
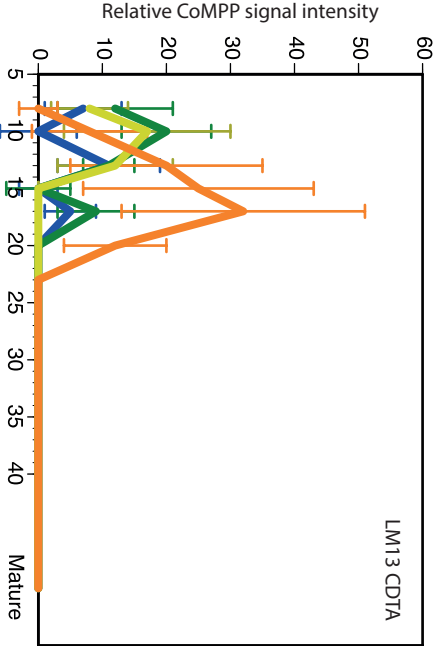
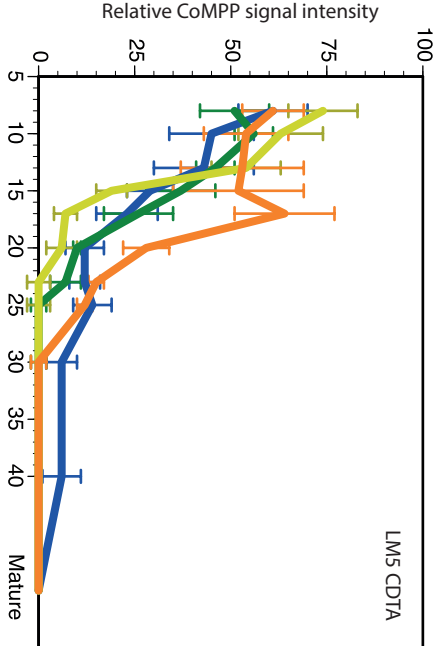
XXT2



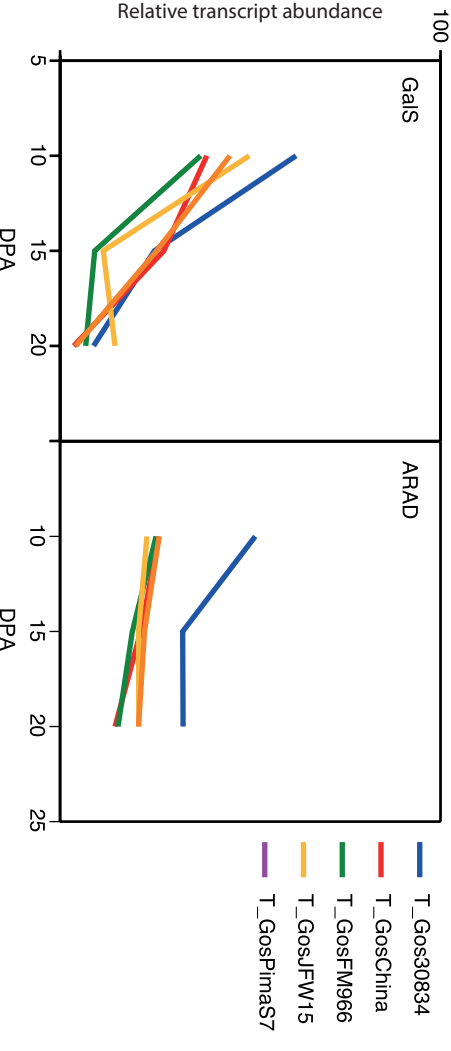
MUR3

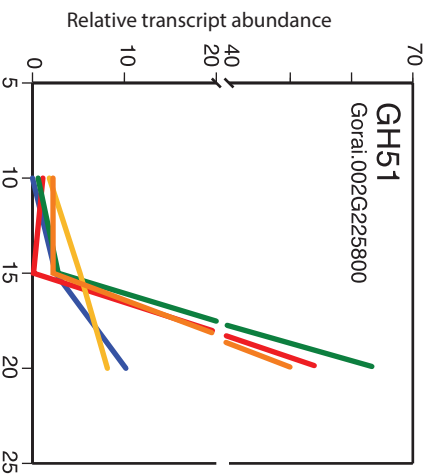




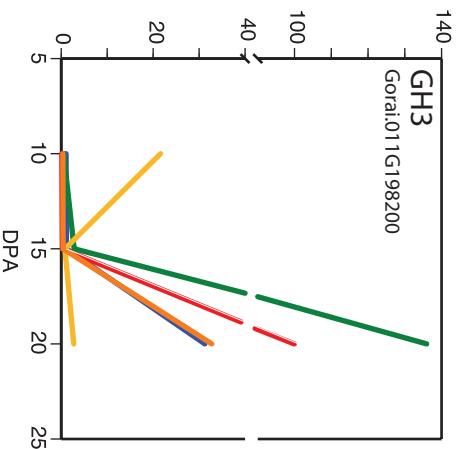
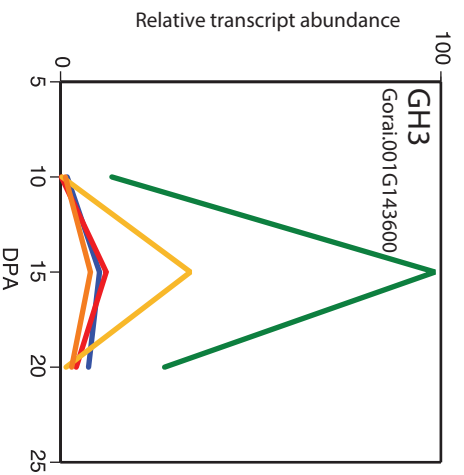
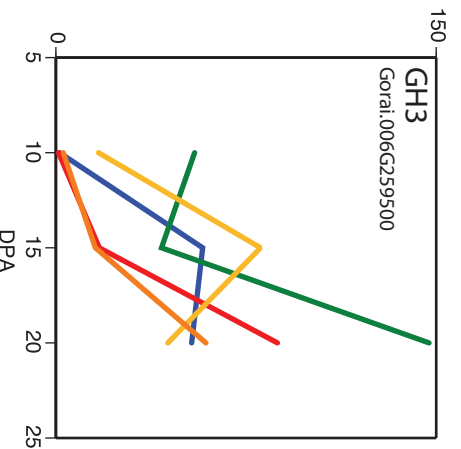
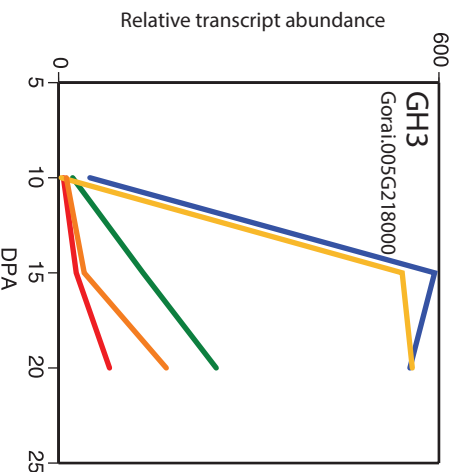


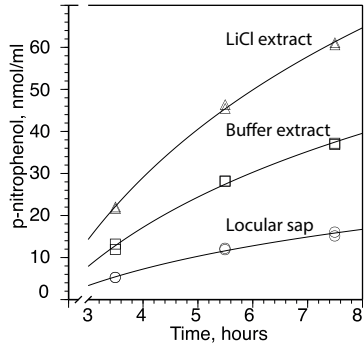
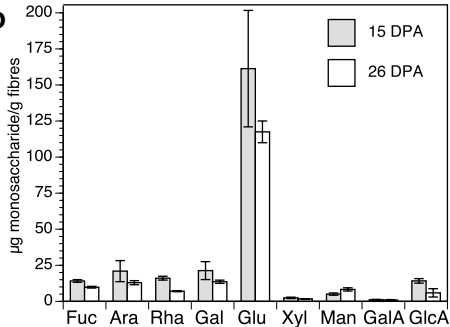
— T_Gos30834
— T_GosFM966
— T_GosJWF15
— T_GosPimaS7





— T_Gos30834
— T_GosChina10
— T_GosFM966
— T_GosJFW15
— T_GosPimaS7



a**b****c**